On the Morphology of (Perfluoroalkyl)alkanes†

Jens Höpken and Martin Möller*

Department of Chemical Technology, University of Twente, P.O. Box 217, 7500 AE Enschede, The Netherlands

Received July 9, 1991; Revised Manuscript Received December 10, 1991

ABSTRACT: The melting and crystallization behavior of (perfluorododecyl)eicosane, $F(CF_2)_{12}(CH_2)_{20}H$, has been investigated by DSC, MAS ^{13}C NMR, and electron microscopic studies. A modification with a higher degree of ordering is obtained when the molecules crystallize from solution. Upon heating, an irreversible transition to a less ordered modification is observed, which is also obtained when the material is cooled from the melt. Electron microscopy reveals the formation of cylindric crystallites of uniform diameter. As an explanation, formation of concentric lamellae is proposed. Different smectic structures were observed for (perfluoroalkyl)alkanes with branched vs linear fluorocarbon segments. Branching in the hydrocarbon segment had no such effect but retarded the crystalline–smectic transition drastically.

Introduction

Structural peculiarities of (perfluoroalkyl)alkanes in the bulk as well as in hydrocarbon and fluorocarbon solution have been reported by others[1-4] and by ourselves.[5] Calorimetric studies demonstrated that the materials undergo at least one, and in some cases even two, solid–solid phase transitions before melting.[1,4,5] Investigation of the molecular packing in different solid phases of the diblock molecules $F(CF_2)_{12}$–$(CH_2)_nH$ with n = 2–20[1,2] and $F(CF_2)_{10}$–$(CH_2)_{10}H$[4] was the subject of Raman and X-ray scattering experiments. From the position of the predominant reflection corresponding to the lamellar spacing, it was concluded that $F(CF_2)_{12}(CH_2)_nH$ with $n \leq 6$ forms monolayer crystals in which the molecules are tilted with respect to the lamella surface below the solid–solid transition and become arranged perpendicular to the lamella surface above the solid–solid transition. Bilayer lamellae crystals were reported for molecules with longer hydrocarbon segments[1-4] and can be explained by the incompatibility of fluorocarbon and hydrocarbon segments of at least six to eight carbons.[3,5] The observed lamellar spacings indicate either a tilted structure or the existence of double-layered lamellae with indented hydrocarbon segments.

Despite ample experimental results, the exact crystal structure of the fluorocarbon–hydrocarbon diblock molecules remains unknown. It is evident from X-ray diffraction that the intermolecular distances within the same lamella correspond to the van der Waals radii of the fluorocarbon segments. However, diffraction spectra obtained for diblock molecules with long alkyl segments did not allow *hkl* indexation.[2] Semiempirical energy calculations to determine the mode of packing of the molecules in the crystal gave similar energy values for different packing models.[2]

In the present paper, we shall present additional information about the thermal behavior and molecular dynamics of (perfluorododecyl)eicosane, $F(CF_2)_{12}(CH_2)_{20}H$. Electron microscopic observations of $F(CF_2)_{12}(CH_2)_{20}H$ crystals are reported, and a model for the molecular organization will be discussed, which can also explain the special gelation behavior of the (perfluoroalkyl)alkanes in hydrocarbon and fluorocarbon solvents.

In a second part, the thermal behavior of fluorocarbon–hydrocarbon molecules with branched segments is presented and the influence of structural irregularities on the different phase transitions is discussed.

* Author to whom correspondence should be addressed.

† Dedicated to Prof. Dr. Bernhard Wunderlich on the occasion of his 60th birthday.

Experimental Section

Materials. All fluorocarbon–hydrocarbon diblock molecules were prepared by free-radical addition of perfluoroalkyl iodides to the corresponding alkene, followed by reduction of the iodide as described previously.[5]

Thermal analysis was performed on a Perkin-Elmer DSC-7 equipped with a PE-7500 computer and TAS-7 software. Cyclohexane, gallium, and indium were used as the calibration standards. Samples of 1 mg and a heating rate of 1 K/min were used to conduct the experiments at conditions close to the thermal equilibrium.

Solid-State MAS ^{13}C NMR spectra were recorded on a Bruker CXP-300 spectrometer at 75.47 MHz as described elsewhere.[6,7]

Scanning electron microscopy was done on a JEOL JSM-T220A instrument. Crystals of (perfluoroalkyl)alkanes, which were obtained by sublimation, were shaded with gold. High magnification images were recorded from freeze–fracture samples with a Hitachi S-800 microscope. The samples were melted between two Cu grids, quenched to −196 °C in liquid propane, and fractured at this temperature. The fracture surfaces were observed directly or were previously shaded with carbon.

Transmission electron microscopy was done on a Philips 400 instrument with an acceleration voltage of 100 kV. The magnification scales were calibrated using crystals of katalase enzyme stained by uranyl acetate. A Balzers BAE 301 freeze–fracture apparatus was used to prepare replicas of the fracture surface of the (perfluoroalkyl)alkanes. Melt-crystallized samples were mounted on a miniature bench vice, cooled to 143 K under high vacuum, and fractured still under vacuum with a moving knife. The resulting fracture surface was shaded unidirectionally, first with platinum under an angle of 45° and then with carbon under an angle of 90°. After the organic material had been removed with Freon 113, the replicas were placed on Cu grids.

Results and Discussion

1. (Perfluorododecyl)alkanes with Different Alkyl Substituents. n-Alkanes with C_{12} fluorocarbon segments, $F(CF_2)_{12}(CH_2)_mH$, can be classified in different groups according to their melting behavior.

i. $F(CF_2)_{12}(CH_2)_mH$ with m = 0 and m = 2 behave similarly to the perfluorinated n-alkanes. At ambient temperature they crystallize in a rhombohedral unit cell with $a = b$ = 5.70–5.73 Å, similar to that of PTFE at temperatures between 30 and 100 °C,[8,9] where there is extensive torsional motion. Although it has not been experimentally confirmed yet, it appears likely that $F(CF_2)_{12}(CH_2)_mH$, m

0024-9297/92/2225-2482$03.00/0 © 1992 American Chemical Society

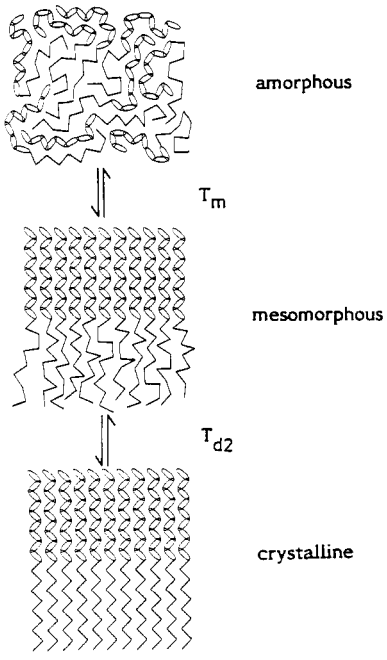

Figure 1. Schematic representation of the stepwise conformational disordering of $F(CF_2)_{12}(CH_2)_mH$, m = 4–14, upon phase transformations. The picture is not meant to represent the actual structure with respect to inclination and crystal conformation.

= 0 or 2, exhibits at least one additional crystal–crystal transition below 173 K which has been reported for $F(CF_2)_{12}F$[10,11] and $F(CF_2)_{20}F$[12-14] and which has been assigned to the onset of rotational motion, helix reversal, and longitudinal displacements.

ii. $F(CF_2)_{12}(CH_2)_mH$ with $4 \leq m \leq 14$ shows in addition to the melting endotherm two other endothermic transitions at temperatures from 147 to 216 K and from 314 to 363 K.[5] The mesomorphic state below the melting (isotropization) transition was identified as a smectic liquid crystalline phase. Melting points and melting entropies depend only little on the length of the hydrocarbon segment. In contrast, the temperature and the entropy of the solid–solid transition increase strongly with the number of methylene units in the hydrocarbon segment. This indicates that, at the solid–solid transition, disordering occurs predominantly in the hydrocarbon segment, while the melting transition is dominated by the disordering of the fluorocarbon segment.

While so far Raman spectra did not indicate gauche defects in the alkyl segments above the disordering transition,[1,3] solid-state ^{13}C NMR experiments confirmed a liquidlike conformational equilibrium in the hydrocarbon segments, and it was concluded that the hydrocarbon segments must have liquidlike conformational freedom and mobility already in the mesomorphic phase.[5] A schematic representation of the variation of the molecular conformation upon phase conversion is given in Figure 1.

Conformational disordering of the hydrocarbon segments upon the transition to the smectic mesophase is consistent with the fact that the cross section occupied by hexagonally packed perfluorinated alkanes (28.3 Å^2)[8,11] is about 30% larger than that of hexagonally packed methylene segments (21.1 Å^2).[15]

The molecular origin of the low-temperature solid–solid transition remains unknown. It might be postulated that it corresponds to the disordering transition observed for perfluorododecane and perfluoroeicosane, which has been assigned to the onset of segmental motion.[9,11-14] High-

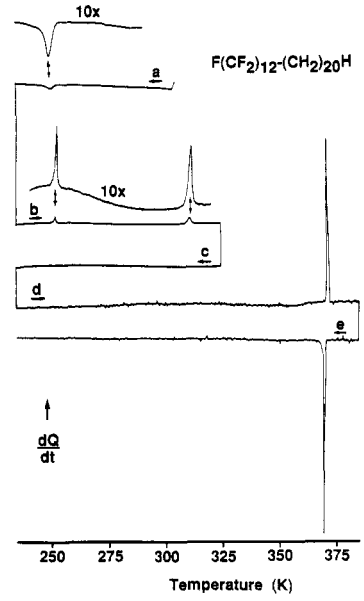

Figure 2. Subsequently recorded DSC traces of $F(CF_2)_{12}(CH_2)_{20}H$ crystallized from toluene solution upon (a) cooling from 303 to 230 K, (b) heating from 230 to 323 K, (c) cooling from 323 to 230 K, (d) heating from 230 to 383 K, and (e) cooling from 383 to 230 K.

power proton-decoupled solid-state ^{13}C NMR experients demonstrated that the chain conformation of the hydrocarbon segment is not changed significantly at this transition. Currently high-power fluorine decoupling is employed to investigate a possible change in the packing of the fluorocarbon segments at this transition.[16]

iii. No transitions other than the melting endotherm were observed for $F(CF_2)_{12}(CH_2)_mH$ with m = 16 and 18 above 170 K. Correspondingly, melting entropies are considerably higher than measured for the compounds with shorter alkyl segments. ΔS_{fusion} per carbon atom results to 4.5 J/(mol K). This value is considerably lower than would be expected for melting of a fully ordered crystal; i.e., ΔS_{conf} of 9.5 J/(mol K) has been calculated for each mole of bonds around which conformational freedom is attained on fusion.[17] It is even lower than the value found for the transition of PTFE from the hexagonal state to the isotropic melt, i.e., ΔS = 5.7 J/(mol K) per carbon. This comparison demonstrates that considerable disorder is retained when $F(CF_2)_{12}(CH_2)_mH$ with m = 16 or 18 is cooled below its melting point. It has yet not been reported whether there is a crystal disordering transition which might correspond to the low-temperature transition and the onset of rotational motion mentioned above.

iv. Again, a different behavior is observed by DSC measurements between 170 and 400 K for $F(CF_2)_{12}(CH_2)_{20}H$ and will be discussed below.

2. (Perfluorododecyl)eicosane. The phase behavior of $F(CF_2)_{12}(CH_2)_{20}H$ depends on the thermal history of the sample. Melt-crystallized material only shows a melting endotherm at 373 K, while solution-crystallized material can exhibit a very complex melting behavior. Figure 2 shows the DSC traces of $F(CF_2)_{12}(CH_2)_{20}H$ crystallized from toluene solution at room temperature. Upon cooling, a reversible and reproducible solid–solid transition was observed. Upon heating for the first time above room temperature, a second but irreversible phase transition was found at 308 K. After the sample underwent the second transition, neither the endotherm at 250 K nor that at 308 K was observed any more and the sample behaved like melt-crystallized material, showing only the melting endotherm. For all compounds $F(CF_2)_{12}(CH_2)_mH$

Table I
Thermal Transitions of $F(CF_2)_{12}(CH_2)_{20}H$, (A) Crystallized from Solution and (B) Crystallized from the Melt

	T_{d1}, K	ΔH, kJ/mol	ΔS, J/K·mol	T_{d2}, K	ΔH, kJ/mol	ΔS, J/K·mol	T_m, K	ΔH, kJ/mol	ΔS, J/K·mol
A	250	4	17	308	8	26	373	60	160
B							373	59	157

with $m \geq 6$ we found melting temperatures 3–5 K above those reported before,[1,2] while the melting entropies agreed very well. In the case of $F(CF_2)_{12}(CH_2)_{20}H$, we observed a T_m of 373 K (vs 369 K) and a ΔH_m of 58 kJ/mol (vs 43 kJ/mol).[1,2]

Apparently, $F(CF_2)_{12}(CH_2)_{20}H$ can crystallize in two different modifications. Crystallization from solution at temperatures below 308 K yields a modification, which undergoes a reversible solid–solid phase transition at 250 K. Table I lists the transition temperatures with the corresponding heats of transition. Molar transition entropies have been calculated by assuming equilibrium transitions and $\Delta S = \Delta H/T$. Because of the observation that the heat of fusion is practically identical for the melt-crystallized and the solution-crystallized modifications ($\Delta H_m = 59$ kJ/mol), the solution-crystallized modification is the thermodynamically stable one according to the enthalpy difference of the 308 K transition ($\Delta H_{d2} = 8$ kJ/mol). At 308 K, this modification transforms into another, less ordered, one. Retransformation upon cooling appears to be kinetically hindered in the absence of solvent.

Solid-state ^{13}C NMR experiments were performed to investigate the molecular processes that occur during the phase transitions. MAS ^{13}C NMR on *n*-alkanes has been shown to give valuable information about variations in the molecular packing, i.e., hexagonal, orthorhombic, or monoclinic subcells, and upon trans–gauche isomerism.[18] Figure 3 shows high-resolution solid-state ^{13}C NMR spectra of solution-crystallized $F(CF_2)_{12}(CH_2)_{20}H$, recorded at increasing temperatures after the sample was cooled to 230 K. The assignment was done according to ref 5. A reversible splitting of the resonance signal of the inner methylene carbons at ~33 ppm was observed when the sample was cooled below 250 K (see Figure 3a–c). This corresponds to the reversible phase transition observed by DSC at this temperature. The small difference in the isotropic chemical shift indicates two different packing geometries which are resolved for the alkyl groups below 250 K. Conformational disordering of the alkyl segment should result in a 2.2 ppm upfield shift.

As shown in Figure 3b,d, a 0.2–0.4 ppm upfield shift was observed for the resonances of the β-CH_2 and α-CH_2 carbons from 34.1 (280 K) to 33.9 ppm (330 K) and from 24.5 (280 K) to 24.1 ppm (330 K), respectively. When solution-crystallized $F(CF_2)_{12}(CH_2)_{20}H$ was heated for the first time above 308 K, the nonreversible phase transition was observed in the DSC experiments. The upfield shift as well as a considerable sharpening of the signals can be explained by an increasing number of gauche defects, indicating further loss of order at the ends of the alkyl segments.[6]

When the sample was cooled from 330 to 230 K, only a weak splitting of the main resonance was observed (Figure 3e). While the transition was irreversible during DSC measurements, the partial reversibility in the solid-state ^{13}C NMR experiments may be caused by pressure built up due to the fast rotation of the sample, which can enhance annealing.

As shown in Figure 3f, the resonances of the inner methylene units were shifted further upfield by 3 ppm at the melting transition. At 370 K, solid and molten forms of

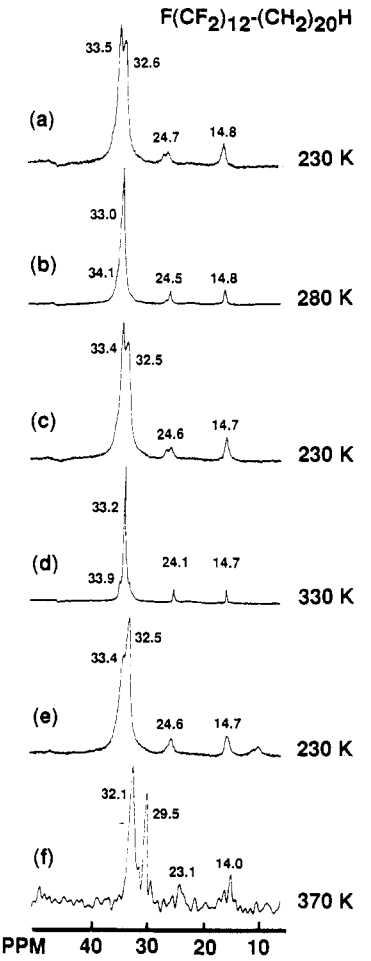

Figure 3. MAS ^{13}C NMR spectra of solution-crystallized $F(CF_2)_{12}(CH_2)_{20}H$ recorded at different temperatures in consecutive order: (a) below the transition at 250 K; (b) above the reversible transition at 250 K, but still below the irreversible transition at 308 K; (c) cooled back below the reversible transition; (d) heated above the irreversible transition at 308 K; (e) cooled below 250 K again (only a weak splitting of the main resonance is observed); (f) at 370 K solid and molten $F(CF_2)_{12}(CH_2)_{20}H$ coexist.

$F(CF_2)_{12}(CH_2)_{20}H$ coexist. The signal at 32.1 ppm is attributed to the solid phase, that at 29.5 ppm to the melt.

It can be summarized that DSC experiments indicate crystallization in two polymorphs. Solid-solid NMR experiments demonstrate further that the structure and packing of the $(CH_2)_{20}H$ segment are not uniform and depend on the temperature. The isotropic chemical shift indicates a predominantly all-trans conformation of the alkyl segments and differences in the packing.

So far, it has not been possible to perform X-ray diffraction experiments that yield clear evidence on the crystal structure. Rabolt et al. reported SAXS and WAXD investigations, which basically gave broad diffraction peaks indicating a hexagonal packing of the perfluoro segments with a long periodicity of 6.3 nm.[1,2] In addition, a broad reflection corresponding to a periodicity of 20–25 nm has been found for which no further explanation could be given.

Macroscopically, it appears that the material can be well crystallized to relatively large crystals of decent quality. As is shown in Figure 4a, the crystals have a fibrillar morphology. The bundles are well aligned unidirectionally, and each bundle appears to consist of several fibrils. The scanning electron microphotograph shown in Figure 4b demonstrates that a fibrillar morphology is still observed at a much smaller scale than can be resolved in Figure 4a. Also, our own X-ray experiments on such

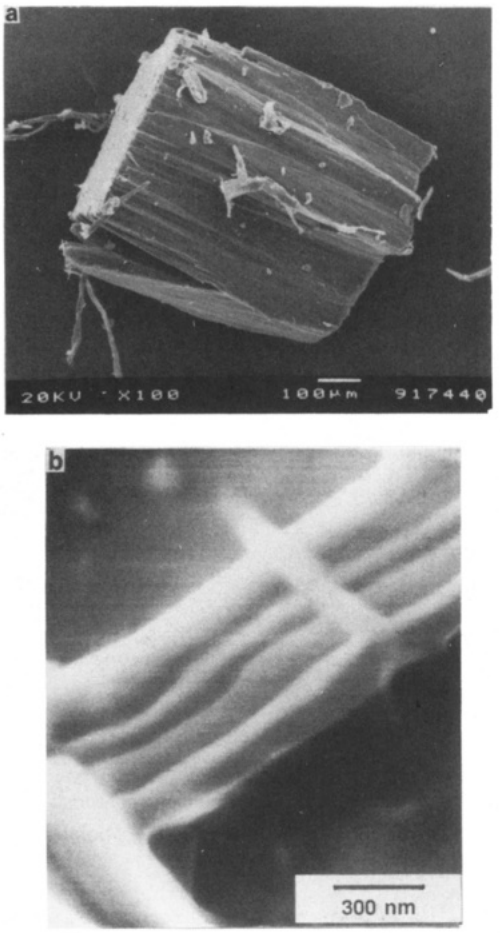

Figure 4. Scanning electron microscopy images of $F(CF_2)_{12}(CH_2)_{20}H$: (a) crystal obtained by sublimation and (b) from a freeze–fractured sample quenched from the melt.

samples did not give diffraction patterns leading to a clearer picture of the molecular organization within the lamellae.

The contour length of $F(CF_2)_{12}(CH_2)_{20}H$ results to 41.33 Å,[4] which is about two-thirds of the long period observed by SAXS experiments. Thus, even the packing of the individual lamellae should be well resolvable by transmission electron microscopy. Figure 5a shows a transmission electron micrograph of a platinum/carbon replica taken from a freeze–fractured $F(CF_2)_{12}(CH_2)_{20}H$ surface of a melt-crystallized sample. The dominant periodical distance of the stripes in the lower right corner is 24 nm. This is 4 times as much as the long period from X-ray diffraction. A second striped structure, much narrower than the first one, can be distinguished in the upper left corner of Figure 5a. Here, the periodical distance is 6 nm, which corresponds to the layer spacing found by X-ray scattering experiments.[1,2] This spacing has been explained by the formation of double-layered lamellae with indented hydrocarbon segments. However, only small sections of the replica show the narrow lamellar structure, while vast areas of the wide-striped structure were found.

Figure 5b shows that the periodical distance of 24 nm does not originate from a lamellar structure but from the surface of a layer of cylinders which have a uniform diameter of 24 nm. From Figure 5a,b it appears that the two periodicities do not belong to the same structural units. So far it has not been possible to obtain the corresponding micrographs from solution-crytallized material and to check whether there is a difference in the fraction of the 6- and 24-nm arrangements.

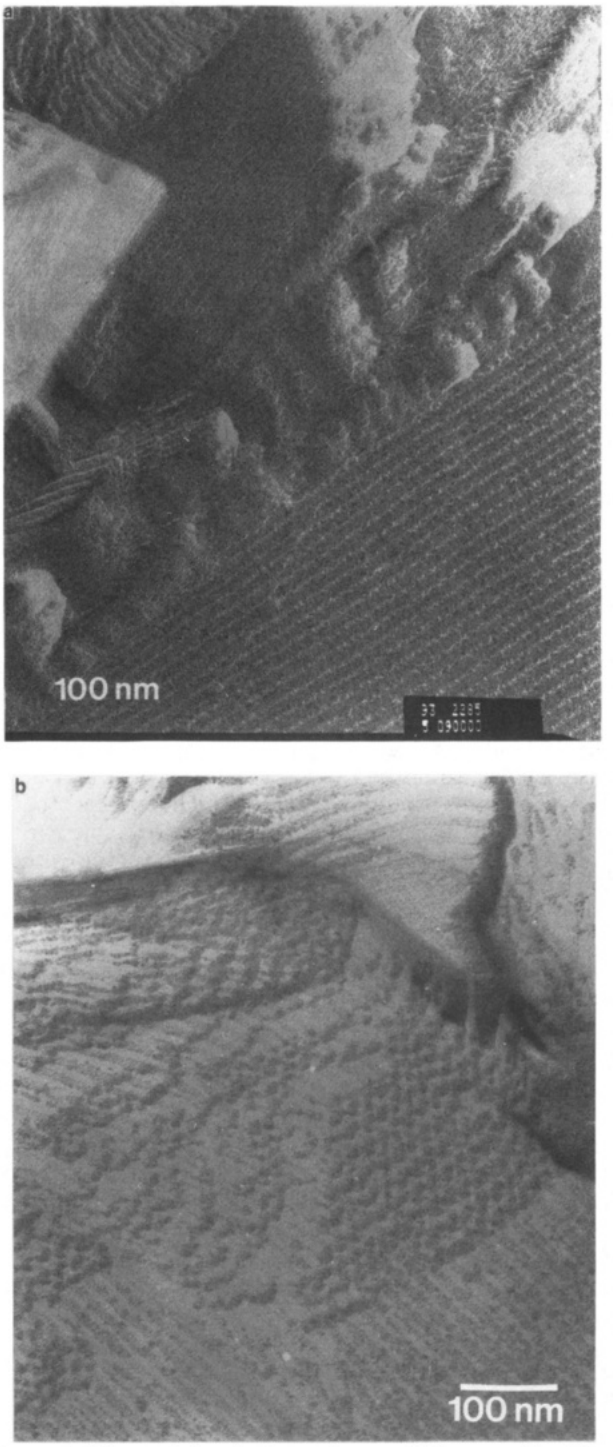

Figure 5. Transmission electron micrograph from a replica taken from a freeze–fracture surface of melt-crystallized $F(CF_2)_{12}$-$(CH_2)_{20}H$. Part a shows besides 24-nm stripes also 6-nm stripes. In part b, it can be seen that the 24-nm stripes are formed by layers of cylinders.

In the following, we want to propose a model to explain the observation of cylinders with a uniform diameter of 24 nm. The following arguments can be considered for the formation of cylinders.

While the cross section of an all-trans planar (orthorhombic) zigzag $(CH_2)_n$ chain[12] is 18.5 Å^2, the cross section of hexagonally packed $(CF_2)_n$ chains[11] resulted to 28.3 Å^2. This difference causes problems for a regular packing of $F(CF_2)_n(CH_2)_mH$ molecules in straight lamellae. A kink in the molecules at the CF_2–CH_2 link resulting in different tilting of the alkyl and the perfluoroalkyl segment can solve the packing problem at least partly. Another or

additional solution can be given by bending of the lamellae, ultimately leading to concentric cylinders.

Formation of cylindrical crystallites is well-known for some silicates such as asbestos[19-21] or imogolite.[22,23] Also in this case, it is the decrease in curvature ($1/r$) with increasing radius which controls the growth in thickness rigorously.

Considering the morphological analogy with asbestos, a concentric or spiralized single-layer structure can be suggested as a model for the packing of $F(CF_2)_{12}(CH_2)_{20}H$. If the cylinders would be made up of single layers with all hydrocarbon segments oriented toward the center, a cylindrical structure becomes logical as a consequence of the different cross sections of the fluorocarbon and hydrocarbon segments. Assuming the molecules are extended (ca. 4 nm), three concentric layers form a 24 nm thick cylinder as observed by electron microscopy. In first approximation, the packing in any layer is determined by its point of highest density, i.e., at the inside of the alkyl and perfluoroalkyl portions. Starting with the fluorocarbon segments in the outermost layer of a 24 nm thick cylinder, the inside border of the fluorocarbon layer would be located at ca. 10.5 nm from the center and the inside border of the connected hydrocarbon layer at ca. 8 nm. The specific area difference between these two shells results to 32%, which accounts for at least part of the 50% difference in the cross sections of the two segments. The second layer would be the least strained, as the specific area difference would be 62%, which is close to the expected density difference. The innermost layer cannot be analyzed on this basis. Thus, a limitation of the cylinder diameter occurs naturally in this model. Unstable structures result when the curvature becomes too small to compensate for the difference in the volume occupied by hydrocarbon and by fluorocarbon segments, as it occurs with increasing diameter of the cylinder.

However, a monolayer arrangement of the molecules is in contradiction to the lamellar spacing of 6.3 nm observed in X-ray experiments.

On the basis of the lamella distance of 6.3 nm which was obtained by Rabolt in X-ray studies on $F(CF_2)_{12}(CH_2)_{20}H$, it has to be assumed that the cylinders are made up of concentric double-layer lamellae as shown in Figure 6; 24 nm corresponds roughly to 4 times the 6.3-nm distance that has been assigned to an indented double layer. In the SAXS experiments it had been noted that $F(CF_2)_{12}(CH_2)_{20}H$ showed not only a relatively sharp single reflection corresponding to d = 6.3 nm but also a broad scattering maximum at smaller angles corresponding to d = 20–25 nm. For a cylinder that is formed from two concentric double layers as shown in Figure 6, the diameter should be roughly 4 times 6 nm. With regard to a particular molecular packing the bending can only be optimal in one of the concentric layers. The wide-angle X-ray diffraction was lacking discrete reflections from particular lattice planes and resembled more amorphous than crystalline materials.[1,2] This diffusity of the WAXD spectrum would be consistent with a cylindrical structure with a gradual change of the packing as the bending of the lamella decreases with increasing diameter of the cylinder.

In a two-bilayer cylinder, 80% of the material is located in the outer layer. Further, it is a general observation for all of the perfluoroalkylalkanes that the crystalline packing is dominated by the perfluoroalkyl segment,[1,2] so it may well be possible that the overall structure is dominated by the favorable packing in the outer bilayer. In this case it has to be assumed that the two layers of alkyl chains in each bilayer are packed differently. To answer these questions, it remains important to investigate whether different lamellar spacings are found for the different modifications observed for $F(CF_2)_{12}(CH_2)_{20}H$ in the DSC and MAS ^{13}C NMR experiments described above.

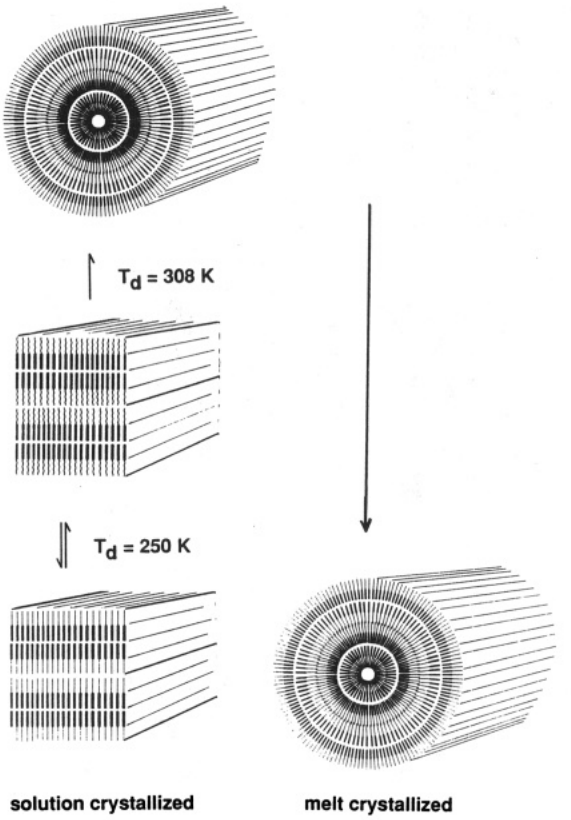

Figure 6. Hypothetical model for the morphology in different modifications of $F(CF_2)_{12}(CH_2)_{20}H$.

On the basis of a bilayer lamella morphology, we propose a hypothetical model for the morphology in different modifications of $F(CF_2)_{12}(CH_2)_{20}H$ which is shown in Figure 6 and which might explain the experimental results obtained from thermal analysis, solid-state ^{13}C NMR, and electron microscopy experiments.

From thermal analysis, it resulted that a modification with a higher degree of overall order results when the material is crystallized from solution compared to that obtained with crystallization from the melt. This modification undergoes a reversible phase transition at 250 K, and at 308 K it transforms to a modification which behaves identically with melt-crystallized samples. Since the replicas observed in the electron microscope have been taken from freeze–fractures of melt-crystallized samples, the dominant cylindric structure should correspond to the thermodynamically less stable modification which does not undergo any phase transitions before melting. Consequently, it is reasonable to assign the straight lamellar morphology with a periodicity of 6 nm to the better ordered modification as obtained by crystallization from solution. At the reversible phase transition at 250 K, disordering occurs in the hydrocarbon segments, which is reflected in the reversible changes observed in the solid-state ^{13}C NMR spectra reported above. At the transition observed at 308 K, the straight lamella bend to form concentric lamellae, which leads to the cylindric morphology observed in the electron micrographs. It is probable that the degree of overall order is lower in the cylindrical morphology, especially when the cores of the cylinders are considered. Less order may be favorable for the arrangement of the hydrocarbon segments which are already in a state of

Figure 7. Electron micrograph from a replica taken from a freeze–fracture surface of melt-crystallized $F(CF_2)_{12}(CH_2)_{14}H$; width of the stripes is 5 nm.

enhanced conformational freedom and rotational mobility. Restoring of the straight lamellar morphology when the cylindric structure is cooled would require displacement of the molecules over large distances. Such process should be kinetically hindered, resulting in the irreversibility of the transition at 308 K.

Formation of needle crystals with extreme aspect ratios is also typical for the (perfluoroalkyl)alkanes $F(CF_2)_{12}(CH_2)_mH$ with $m = 6–14$. Electron microscopic studies on those, however, did not show a regular cylindrical structure as described above. Figure 7 shows a replica from a freeze–fracture surface of $F(CF_2)_{12}(CH_2)_{14}H$. Structures on the mountain-type morphology correspond well with the 5 nm long period from SAXS experiments.[1,2] To explain the formation of needle crystals upon crystallization from solution, another, but for the case of $F(CF_2)_{12}(CH_2)_{20}H$ probably complementary, aspect has to be considered. As discussed above, DSC experiments on (perfluorododecanoyl)alkanes with less than 14 methylene units gave a phase transition below isotropization, which was assigned to considerable conformational disordering of the hydrocarbon segment. Thus, at a temperature just below the melting point only the fluorocarbon segments are packed regularly and have a uniform conformation. The hydrocarbon segments are still mobile and conformationally disordered. Therefore, the crystallite growth must occur predominantly by aggregation of fluorocarbon segments to a double layer. Also in this case, the double layer bends because of the difference in the cross sections of the fluorocarbon and the hydrocarbon segment. Crystallite growth in the direction parallel to the lamella surface requires the deposition of fluorocarbon segments onto an ordered fluorocarbon surface and should be fast. In contrast, growth perpendicular to the lamella surface requires the deposition of mobile hydrocarbon segments onto a conformationally disordered hydrocarbon surface. Thus, the diameter of the crystallites should increase very slowly.

It is the peculiar, enormous aspect ratio of the needle crystallites of (perfluoroalkyl)alkanes by which gelation is to be explained as observed when a hot solution is cooled in hydrocarbon or fluorocarbon solvent. Extremely long, thin crystallites build up a fine network in which up to 98% of solvent can be enclosed. The macroscopic aspect is a solidification of the whole system to an opaque gel. In contrast to other studies[24] we did not find any indication for a considerable difference in the crystal structures of the gel phase and the solid state.[5]

3. (Perfluoroalkyl)alkanes with Branched Segments. The previous discussion demonstrated variations in the melting behavior and the occurrence of mesomorphic phases in dependence of the length of the hydrocarbon segment. For $F(CF_2)_n(CH_2)_mH$ compounds with $n = 10$ or 12 and $m = 4–14$, it was pointed out that the isotropization transition can be explained on the molecular scale by the breakdown of the regular fluorocarbon segment packing, while the hydrocarbon segments are already in a liquidlike conformationally disordered state.

Assignment of the thermal transitions to the onset of disordering of particular segments may be also confirmed by investigation of fluorocarbon–hydrocarbon molecules with branched segments. With respect to the discussion above, branching in the hydrocarbon segment should, in a first approach, lead to depression of the mesophase transition. Branching in the fluorocarbon segment can be expected to effect predominatly the isotropization transition.

Table II represents DSC data for $F(CF_2)_{12}CH_2CH(CH_3)(CH_2)_9H$ and $(CF_3)_2CF(CF_2)_4(CH_2)_mH$ with $m = 10$ or 12 in comparison to (perfluoroalkyl)alkanes with the corresponding linear hydrocarbon or fluorocarbon segment.

Figure 8 shows crystals of $F(CF_2)_{12}CH_2CH(CH_3)(CH_2)_9H$ that were obtained by sublimation under high-vacuum conditions. They have the shape of cigars with a round perimeter and can be several millimeters long. The clear crystals are birefringent. The crystals are very soft and can easily be bent by a slight mechanical force. In contrast, sublimation of $F(CF_2)_{12}(CH_2)_{12}H$ and other linear diblock compounds only gave microcrystalline powders. This different behavior is explained by the low mesomorphic transition temperature of $F(CF_2)_{12}CH_2CH(CH_3)(CH_2)_9H$. During the sublimation, evaporation and deposition take place while the material is in the highly mobile mesomorphic state. Defects in the partially ordered structure can heal, which leads to the formation of large crystals. While the stability of the liquid crystalline phase was drastically increased by the introduction of a methyl branch into the hydrocarbon segment, no alteration of the structure of the mesomorphic phase was observed. Figure 9a shows the polarization microscopic texture obtained for $F(CF_2)_{12}CH_2CH(CH_3)(CH_2)_9H$ in the mesomorphic state. The same type of bâtonnet texture was also observed for all linear (perfluoroalkyl)alkanes.[3–5]

The mesomorphic and melting transitions of compounds of the type $(CF_3)_2CF(CF_2)_n(CH_2)_mH$ were observed only 10–15 K lower than those of the linear molecules having the same hydrocarbon segment and a linear but by one carbon atom shorter fluorocarbon segment (Table IIB). As might be expected, branching at one end of the diblock molecules has less effect than an irregularity in the center of the molecule. Figure 9b shows the texture observed by polarization microscopy for $(CF_3)_2CF(CF_2)_6(CH_2)_{10}H$ in the mesomorphic state. The texture can be described as of the broken focal conic type. In contrast, bâtonnet textures were always obtained for compounds with linear fluorocarbon segments, even when the hydrocarbon segment was branched as described above.

The variation in the texture is another indication that in the mesomorphic state only the fluorocarbon segments are regularly packed, while the hydrocarbon portions are already mobile and conformationally disordered. Con-

Table II
Comparison of the Thermal Data of Linear and Branched Fluorocarbon–Hydrocarbon Molecules

		T_d, K	ΔH_d, kJ/mol	ΔS_d, J/K·mol	T_m, K	ΔH_m, kJ/mol	ΔS_m, J/K·mol
A	$F(CF_2)_{12}CH_2CH(CH_3)(CH_2)_9H$	260	9	33	347	25	72
	$F(CF_2)_{12}(CH_2)_{10}H$	342	10	28	365	26	71
	$F(CF_2)_{12}(CH_2)_{12}H$	352	10	30	364	26	71
B	$(CF_3)_2CF(CF_2)_4(CH_2)_{10}H$	220	3	14	261	18	66
	$F(CF_2)_8(CH_2)_{10}H$	288	4	12	308	20	65
	$(CF_3)_2CF(CF_2)_6(CH_2)_{10}H$	274	1	4	298	25	82
	$F(CF_2)_{10}(CH_2)_{10}H$	317	4	13	337	24	73
	$(CF_3)_2CF(CF_2)_6(CH_2)_{12}H$				310	34	110
	$F(CF_2)_{10}(CH_2)_{12}H$	334	6	19	338	27	80

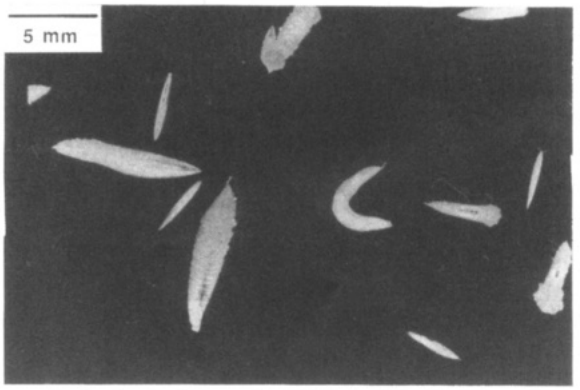

Figure 8. Optical micrograph of $F(CF_2)_{12}CH_2CH(CH_3)(CH_2)_9H$ crystals between crossed polarizers. One crystal was bent to demonstrate the soft consistency of the material in the mesomorphic phase.

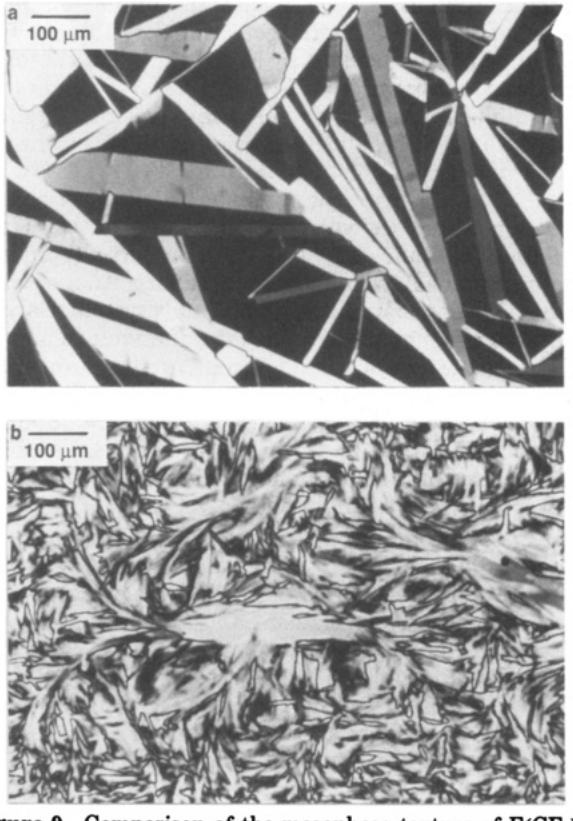

Figure 9. Comparison of the mesophase texture of $F(CF_2)_{12}CH_2CH(CH_3)(CH_2)_9H$ at 346 K (a) and of $(CF_3)_2CF(CF_2)_6(CH_2)_{10}H$ at 293 K (b) as observed by optical microscopy between crossed polarizers.

sequently, the introduction of an irregularity into the structure of the fluorocarbon segment can cause a change of the mesomorphic phase structure, while branching in the hydrocarbon segment leaves the structure unchanged.

Conclusions. The behavior of fluorocarbon–hydrocarbon molecules is governed by their amphiphilic character, which arises from the incompatibility of the constituent segments. Fluorocarbon and hydrocarbon segments segregate upon crystallization, which leads to the formation of double-layered lamellar structures. However, dense packing of the molecules within the lamellae remains mysterious from the principal reason that the cross section of the fluorocarbon segment (28.3 Å^2) exceeds by far that of the hydrocarbon segment (18.5 Å^2). Antiparallel packing modes as proposed from semiempirical force field calculations are highly contradictory to the demixing of fluorocarbon–hydrocarbon molecules, and X-ray scattering experiments did not yield a conclusive picture.[1,2] Molecular organization of fluorocarbon–hydrocarbon molecules within straight lamellae structures appears to be a too simple concept.

Electron microscopy experiments gave evidence for a fibrillar morphology with one preferential orientation in the case of $F(CF_2)_{12}(CH_2)_{20}H$. On the molecular scale, concentric tubular lamellae of uniform diameter were observed. Both models presented imply a gradual change of the packing, especially of the fluorocarbon segments with increasing diameter of the cylinder. The absence of strictly defined intermolecular distances is reflected in the broad X-ray diffraction signals obtained by Rabolt and co-workers.[1,2] An ordered arrangement should be difficult in the central part of the cylinder. DSC experiments showed that a higher degree of order is achieved when $F(CF_2)_{12}(CH_2)_{20}H$ is crystallized in the presence of solvent. Solid-state ^{13}C NMR spectra of solution-crystallized material resolved two different conformations of the hydrocarbon segments at temperatures below 250 K. Above 308 K, $F(CF_2)_{12}(CH_2)_{20}H$ converts irreversibly to a less ordered modification.

Results of investigations on (perfluoroalkyl)alkanes with branched hydrocarbon or fluorocarbon segments supported the concept of conformational disorder and mobility in the hydrocarbon portion already in the mesomorphic state. Branching of the fluorocarbon segment led to a change of the lamellar structure of the smectic phase. No structural change of the liquid crystalline phase was observed upon introduction of a branch into the hydrocarbon segment in β-position to the fluorocarbon segment. On the other hand, packing of the branched hydrocarbon segment upon cooling of the mesomorphic phase was drastically retarded.

Large birefringent crystals of the material were obtained by sublimation, when evaporation and deposition took place within the temperature range of the mesomorphic phase.

Acknowledgment. Valuable discussions with Dr. B. Lotz are gratefully acknowledged. We thank Dr. M. Kunz

and C. Åhnelt (University of Freiburg, Germany) for electron microscopic work and D. Oelfin for performing the solid-state NMR experiments. Financial support for J.H. was provided by the Max Buchner Stiftung.

References and Notes

(1) Rabolt, J. F.; Russell, T. P.; Twieg, R. J. *Macromolecules* **1984**, *17*, 2786.
(2) Russell, T. P.; Rabolt, J. F.; Twieg, R. J.; Siemens, R. L.; Farmer, B. L. *Macromolecules* **1986**, *19*, 1135.
(3) Mahler, W.; Guillon, D.; Skoulios, A. *Mol. Cryst. Liq. Cryst., Lett.* **1985**, *2*, 111.
(4) Viney, C.; Russell, T. P.; Depero, L. E.; Twieg, R. J. *Mol. Cryst. Liq. Cryst.*, **1989**, *168*, 63.
(5) Höpken, J.; Pugh, C.; Richtering, W.; Möller, M. *Makromol. Chem.* **1988**, *189*, 911.
(6) Möller, M.; Cantow, H. J.; Drotloff, H.; Emeis, D.; Lee, K. S.; Wegner, G. *Makromol. Chem.* **1986**, *187*, 1237.
(7) Drotloff, H.; Rotter, H.; Emeis, D.; Möller, M. *J. Am. Chem. Soc.* **1987**, *109*, 7797.
(8) Dorset, D. L. *Chem. Phys. Lipids* **1977**, *20*, 13.
(9) Starkweather, H. W.; Zoller, P.; Jonas, G. A.; Vega, A. J. *J. Polym. Sci., Polym. Phys. Ed.* **1981**, *20*, 751.
(10) Starkweather, H. W. *Macromolecules* **1986**, *19*, 1131.
(11) Strobl, G. R.; Schwickert, H.; Trzebiatowski, T. *Ber. Bunsen-Ges. Phys. Chem.* **1983**, *87*, 274.
(12) Schwickert, H.; Strobl, G. R.; Kimmig, M. *J. Chem. Phys.* **1991**, submitted for publication.
(13) Albrecht, T.; Elben, H.; Jaeger, R.; Kimmig, M.; Steiner, R.; Strobl, G. R.; Stühn, B.; Schwickert, H.; Ritter, C. *J. Chem. Phys.* **1991**, submitted for publication.
(14) Albrecht, T.; Jaeger, R.; Petry, W.; Steiner, R.; Strobl, G. R.; Stühn, B. *J. Chem. Phys.* **1991**, submitted for publication.
(15) Strobl, G. R. *J. Polym. Sci., Polym. Symp.* **1977**, *59*, 121.
(16) Veeman, W. S. Private communication.
(17) Wunderlich, B.; Grebowicz, J. *Adv. Polym. Sci.* **1984**, *60/61*, 1.
(18) Wunderlich, B.; Möller, M.; Grebowicz, J.; Baur, H. *Adv. Polym. Sci.* **1988**, *87*, 1.
(19) Whittaker, E. J. W. *Acta Crystallogr.* **1957**, *10*, 149, and references cited therein.
(20) Yada, K. *Acta Crystallogr.* **1971**, *26*, 659.
(21) Monkman, L. J. In *Fibre Science*; Happey, F., Ed.; Academic Press: New York, 1979; Vol. 3, p 163.
(22) Cradwick, P. D. G.; Farmer, V. C.; Russell, J. D.; Masson, C. R.; Wada, K.; Yoshinaga, N. *Nature* **1972**, *240*, 187.
(23) Donkai, N.; Inagaki, H.; Kajiwara, K.; Urakawa, H.; Schmidt, M. *Makromol. Chem.* **1985**, *186*, 2623.
(24) Twieg, R. J.; Russell, T. P.; Siemens, R. L.; Rabolt, J. F. *Macromolecules* **1985**, *18*, 1361. Twieg, R. J.; Russell, T. P.; Siemens, R. L.; Rabolt, J. F. *Polym. Prepr. (Am. Chem. Soc., Div. Polym. Chem.)* **1986**, *27* (1), 223.

Registry No. $F(CF_2)_{12}(CH_2)_{20}H$, 89109-72-8; $F(CF_2)_{12}CH_2CH(CH_3)(CH_2)_9H$, 116177-49-2; $F(CF_2)_{12}(CH_2)_{10}H$, 93454-72-9; $F(CF_2)_{12}(CH_2)_{12}H$, 89109-71-7; $(CF_3)_2CF(CF_2)_4(CH_2)_{10}H$, 139277-00-2; $F(CF_2)_8(CH_2)_{10}H$, 138472-76-1; $(CF_3)_2CF(CF_2)_6(CH_2)_{10}H$, 139277-01-3; $F(CF_2)_{10}(CH_2)_{10}H$, 90499-29-9; $(CF_3)_2CF(CF_2)_6(CH_2)_{12}H$, 139277-02-4; $F(CF_2)_{10}(CH_2)_{12}H$, 93454-71-8; $F(CF_2)_{12}(CH_2)_{14}H$, 93454-73-0.